

Lawrence Berkeley National Laboratory

Recent Work

Title

NUCLEAR SPIN AND HYPERFINE STRUCTURE OF ^{121}Sn AND ^{113}Sn

Permalink

<https://escholarship.org/uc/item/1tj601xq>

Authors

Prior, Michael H.
Dymanus, Antoni
Shugart, Howard A.
et al.

Publication Date

1968-11-25

cy. 2

RECEIVED
UNIVERSITY OF CALIFORNIA
LIBRARY AND DOCUMENTS SECTION
OCT 31 1968

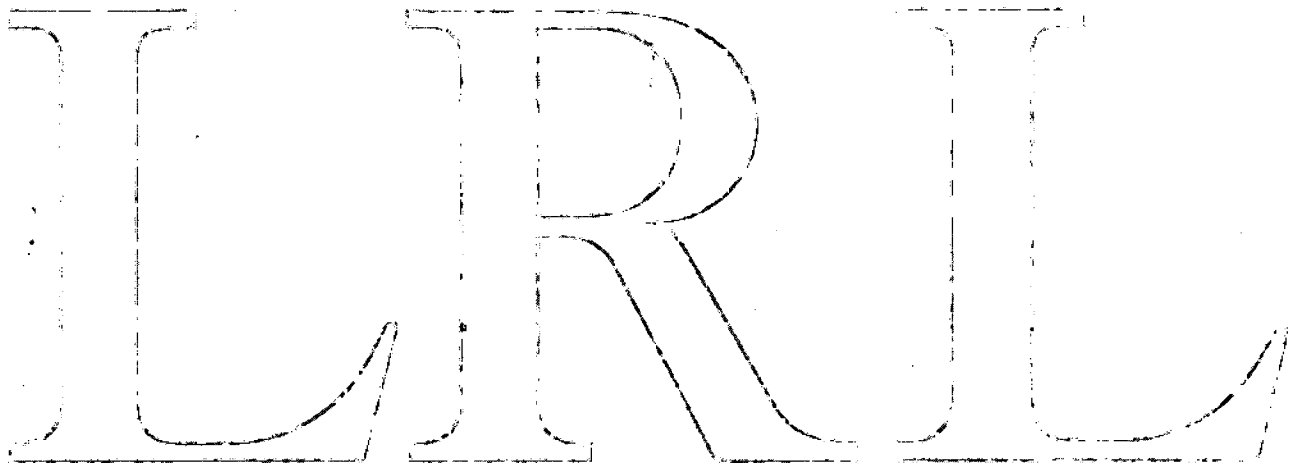
NUCLEAR SPIN AND HYPERFINE STRUCTURE
OF ¹²¹Sn AND ¹¹³Sn

Michael H. Prior, Antoni Dymanus, Howard A. Shugart,
and Paul A. Vanden Bout

November 25, 1968

RECEIVED
LAWRENCE
RADIATION LABORATORY
DEC 3
LIBRARY
DOCUMENTS

TWO-WEEK LOAN COPY
This is a Library Circulating Copy
which may be borrowed for two weeks.
For a personal retention copy, call
Tech. Info. Division, Ext. 5545



LAWRENCE RADIATION LABORATORY
UNIVERSITY of CALIFORNIA BERKELEY

DISCLAIMER

This document was prepared as an account of work sponsored by the United States Government. While this document is believed to contain correct information, neither the United States Government nor any agency thereof, nor the Regents of the University of California, nor any of their employees, makes any warranty, express or implied, or assumes any legal responsibility for the accuracy, completeness, or usefulness of any information, apparatus, product, or process disclosed, or represents that its use would not infringe privately owned rights. Reference herein to any specific commercial product, process, or service by its trade name, trademark, manufacturer, or otherwise, does not necessarily constitute or imply its endorsement, recommendation, or favoring by the United States Government or any agency thereof, or the Regents of the University of California. The views and opinions of authors expressed herein do not necessarily state or reflect those of the United States Government or any agency thereof or the Regents of the University of California.

Submitted to The Physical Review

UCRL-18441
Preprint

UNIVERSITY OF CALIFORNIA

Lawrence Radiation Laboratory
Berkeley, California

AEC Contract No. W-7405-eng-48

NUCLEAR SPIN AND HYPERFINE STRUCTURE OF ^{121}Sn AND ^{113}Sn

Michael H. Prior, Antoni Dymanus, Howard A. Shugart,
and Paul A. Vanden Bout

November 25, 1968

NUCLEAR SPIN AND HYPERFINE STRUCTURE OF ^{121}Sn AND $^{113}\text{Sn}^*$

Michael H. Prior[†], Antoni Dymanus[†], Howard A. Shugart
and Paul A. Vanden Bout[‡]

Lawrence Radiation Laboratory and Department of Physics
University of California, Berkeley, California

November 25, 1968

ABSTRACT

We have used the atomic-beam magnetic-resonance technique to measure the nuclear spin I and hyperfine structure interaction constants a and b of 27-hour ^{121}Sn and 118-day ^{113}Sn in the 3P_1 electronic states. From the measured interaction constants we deduce values for the nuclear magnetic-dipole and electric quadrupole moments μ_I and Q . Our results are, for ^{121}Sn : $I = 3/2$, $a = \pm 128.726(8)$ MHz, $b = \pm 32.374(12)$ MHz, $b/a > 0$, from which we deduce $\mu_I(\text{uncorr}) = \mp 0.695(7)$ nm and $Q = \pm 0.08(4)$ b; and for ^{113}Sn : $I = 1/2$, $a = \pm 485.911(25)$ MHz, from which we deduce $\mu_I(\text{uncorr}) = \mp 0.875(9)$ nm.

I. INTRODUCTION

This effort is a part of the continuing program of the Berkeley Atomic Beam Group in the measurement of spins and multipole moments of radioactive nuclei using the atomic-beam magnetic-resonance technique. Such measurements have served well in the past as bench marks and constraints on various theories of nuclear structure. To the extent that current nuclear theories are imperfect, it is hoped that further measurements may shed light on how they may be improved. In the past we have made some effort to extend spin and moment measurements to isotopes lying on both sides of the region of stability for a particular element. The measurements described here were carried out in this spirit. We have measured the nuclear spins and moments and the hyperfine-structure separations of 118-day ^{113}Sn and 27-hour ^{121}Sn in the $(5p^2) \ ^3P_1$ electronic state. These results extend from three to five the number of odd-mass tin isotopes whose spins and moments have been measured.

II. THE ISOTOPES AND THEIR PRODUCTION

^{121}Sn and ^{113}Sn are both radioactive with respective half-lives of about 27 hours and 118 days. ^{121}Sn decays by low-energy beta emission directly to the ground state of stable ^{121}Sb . ^{113}Sn decays primarily (98.2%) by electron capture to the 0.393-Mev isomeric level of ^{113}In , which subsequently decays with 100-minute half-life to the stable ^{113}In ground state. Both isotopes were produced by irradiation of stable Sn metal in a nuclear reactor by the $^A\text{Sn}(n,\gamma)^{A+1}\text{Sn}$ process. For experiments on ^{121}Sn , 1-gram samples were irradiated for 3-day periods in the General Electric reactor at Vallecitos, California. Consideration of cross

sections and relative abundances show that for such an irradiation, during the first week after removal from the core, the predominant activity present in the sample is due to ^{121}Sn . This was confirmed by observation of the decay of the sample. For experiments on ^{113}Sn much longer irradiations were used. Two samples were made. The first consisted of 4 grams of stable Sn irradiated for about 30 days in the AEC reactor at Savannah River, Ga. The second contained 2 grams and was placed in the core of the MTR reactor of the Idaho Nuclear Corporation, also for 30 days. After receiving these samples, we allowed a few weeks for decay of ^{121}Sn before beginning the experiments on ^{113}Sn . At that time none of the other Sn activities produced were significant compared with that of ^{113}Sn .

III. PRODUCTION AND DETECTION OF THE ATOMIC BEAM

The electronic configuration of the ground state of Sn is $5s^2 5p^2$. This configuration yields the five electronic states listed in Table I. Also included are the energies of the states above the ground 3P_0 state, the percentage of the atomic-beam atoms present in each state, and the electronic g factors. It is impossible to deflect significantly the 3P_0 atoms in our beam apparatus; all work reported here was carried out in the metastable 3P_1 state.

The atomic beam was produced by electron bombardment of a tantalum oven containing a carbon crucible and lid. The Sn was placed inside the crucible and the oven was heated to about 1400°C . Sn atoms left the oven through a carbon slit 0.004 in. wide.

Beams of both isotopes were detected by collecting them on clean sulfur surfaces exposed for 5-minute periods at the detector position of

the apparatus. Radioactive counting of the activity on the sulfur surfaces served to measure the beam intensities. In the experiments on ^{121}Sn the beta activity was counted in a low-background anticoincidence-guarded Geiger counter system. Typical background rates were 1 to 2 counts per minute, whereas resonance signals ranged from 20 to 80 counts per minute. The ^{113}Sn activity was measured by counting the 25-keV K x-ray emitted in the electron-capture decay to $^{113\text{m}}\text{In}$. This was done with a conventional NaI scintillator and photomultiplier system. Background and signal rates were similar to those in the ^{121}Sn experiments.

In order to cancel out fluctuations in the atomic beam intensity, two sulfur surfaces were exposed simultaneously during each collecting period. One surface was placed on the beam center line, where signals would appear as an increase in activity collected. The second, a normalization surface, was placed to one side of the center line and received a constant fraction of the beam intensity. The signal was then taken as the ratio of the activities collected on the two surfaces. It is this ratio which is plotted, versus radio frequency, to yield a resonance curve.

IV. THE APPARATUS

The beam apparatus used in these experiments is of the conventional "flop-in" design described in detail elsewhere.¹ On its way to the beam detector an atom passes successively through three magnetic fields denoted A , C , and B oriented transverse to the beam direction. In order for an atom to reach the flop-in detector it must undergo equal and opposite deflections as it passes through the inhomogeneous A and B fields. This will occur only if the atom is made to make a transition in the homogeneous

C field between hyperfine-Zeeman sublevels such that its magnetic moment in B is opposite to that in A . Because the A field and B field are large enough to overcome the coupling of the nuclear angular momentum \underline{I} to the electronic angular momentum \underline{J} , this requirement leads to a magnetic selection rule $m_J(A) = -m_J(B)$ with $m_J \neq 0$, where $m_J = \langle J_z \rangle$. Transitions are induced in the C field by introducing small radio-frequency fields oriented either parallel or perpendicular to the static field. The C -field intensity may be varied to study the field dependence of the energy levels participating in the flop-in resonance signals.

V. GENERAL PRINCIPLES

The Hamiltonian, relevant to these experiments, for an atom with hyperfine structure (hfs) in an external magnetic field \underline{H} is given by

$$\mathcal{H} = \mathcal{H}_{hfs} + \mathcal{H}_Z \quad (1)$$

with

$$\mathcal{H}_Z = -g_J \mu_B \underline{J} \cdot \underline{H} - g_I \mu_N \underline{I} \cdot \underline{H} \quad (2)$$

and in general²

$$\mathcal{H}_{hfs} = \sum_k T^k(n) \cdot T^k(e) \quad (3)$$

In the above, \underline{J} and \underline{I} are the vector electronic and nuclear angular momentum operators, and $g_J = \mu_B/J$ and $g_I = \mu_N/I$ are the electronic and nuclear g factors expressed in Bohr magnetons. The quantity $T^k(n) \cdot T^k(e)$ is the scalar product of the k th-rank hfs tensor operators. $T^k(n)$

operates on the nuclear coordinates and $T^k(e)$ on the electronic coordinates.

Since $\langle T^k(n) \cdot T^k(e) \rangle = 0$ for $k > 2$ [$\min(I, J)$], we need only $k = 1$ and $k = 2$ terms for ^{121}Sn that has $I = 3/2$, $J = 1$; and only the $k = 1$ term for ^{113}Sn with $I = 1/2$, $J = 1$. Furthermore, when the separation of adjacent J states in the atoms is large compared with the hfs, one can write the $k = 1$ (magnetic dipole) and $k = 2$ (electric quadrupole) terms of Eq. (3) as effective operators of order k in the operators $\underline{I} \cdot \underline{J}$, $\underline{I} \cdot \underline{I}$ and $\underline{J} \cdot \underline{J}$. Thus Eq. (3) becomes

$$\mathcal{K}_{hfs} = ha \underline{I} \cdot \underline{J} + hb \frac{[3(\underline{I} \cdot \underline{J})^2 + 3/2(\underline{I} \cdot \underline{J}) - I(I+1)J(J+1)]}{2I(2I-1)J(2J-1)} \quad (4)$$

This formula may be taken as correct for these experiments, considering the precision achieved and the fact that the ratio of the hfs to the separation of adjacent J levels is about 10^{-5} in the Sn isotopes. The hfs constants a and b are related to the nuclear magnetic dipole moment μ_I and nuclear electric quadrupole moment Q by the relations

$$ha = - \frac{\mu_I H_e}{IJ} \quad , \quad (5)$$

$$hb = eq_J Q \quad , \quad (6)$$

where H_e is the atomic magnetic field and q_J is the atomic electric field gradient at the nucleus.

At zero magnetic field an atomic level with quantum number J is split by \mathcal{K}_{hfs} into a number of levels specified by the different values of total angular momenta $\underline{F} = \underline{I} + \underline{J}$ allowed by vector addition rules. In an external field, \mathcal{K}_Z splits each F level into $(2F+1)$ sublevels specified by values of $\langle F_z \rangle = M$; states of the same M but differing in F by ± 1 are mixed by \mathcal{K}_Z so that, to a greater extent as H is increased,

F becomes less a "good" quantum number to describe a state. However, since most atomic-beam magnetic-resonance work begins at near zero C -magnet field, it is customary, when describing radio-frequency transitions, to label a state by its zero-field F and M quantum numbers. In the high fields of the A and B magnets, $\langle \mathcal{H}_Z \rangle \gg hfs$ and the atomic states are near eigenstates of \mathcal{H}_Z best described by their quantum numbers $m_J = \langle J_z \rangle$ and $m_I = \langle I_z \rangle$. Thus when describing beam trajectories these quantum numbers are most commonly used.

In these experiments it was desired to measure the quantities I , a , and b (^{121}Sn only) for the two isotopes studied, from which values of their nuclear moments could be determined. This was done by observation of radio-frequency transitions between various hyperfine-Zeeman sublevels at varying magnetic fields. The transitions observed were magnetic-dipole and hence obeyed the selection rules $\Delta M = 0, \pm 1$ in addition to the machine rule $m_J(A) = -m_J(B)$. The magnitude of the C -magnet field was determined from the observed frequency of the flop-in transition between F, M levels $I+1/2, -I+1/2$ and $I+1/2, -I-1/2$ and the known constants of one of the alkali metals ^{133}Cs , ^{85}Rb , or ^{87}Rb . The particular alkali used varied from one experimental run to another. The quantities I , g_J , μ_I , and a for these calibration isotopes are listed in Table VII.

VI. SPIN MEASUREMENTS

The nuclear spins of ^{121}Sn and ^{113}Sn were measured by observation of rf transitions between low-field Zeeman levels in the hfs states with $F = I + J$. The frequency of this transition is given approximately by

$$\nu = -g_J [J/(I+J)] (\mu_0/h)H \quad (7)$$

Because $J = 1$, a single transition changing M by ± 1 in the C field does not satisfy the machine selection rule $m_J(A) = -m_J(B)$. However, because at low field the Zeeman levels are equally spaced by $h\nu$, it is possible (by application of enough rf power) to induce double quantum transitions yielding $\Delta M = \pm 2$. One

of these transitions corresponds, at the high field of the *A* and *B* magnets, to the transition $m_J = \pm 1 \rightarrow m_J = \mp 1$, thus satisfying the machine selection rule for observation of a flop-in signal. Such double-quantum transitions may be observed with decreasing intensity as *H* is increased, until the low-field approximation of equal level spacing is violated by several resonance line widths.

Figures 1 and 2 show the results of spin searches for ^{121}Sn and ^{113}Sn at magnetic fields of a few gauss. Clear increases in signal above background are indicated at frequencies corresponding to $I = 3/2$ and $1/2$ respectively. Conclusive assignment of the observed $I = 3/2$ to ^{121}Sn was made on the basis of the characteristic 27-hr beta emission decay on the resonance buttons. The long half-life of ^{113}Sn (118 days) precluded a similar decay study extending over several half-lives; however, the decay of resonance buttons extending over many weeks showed no significant departure from a decay with 118-day half-life. Because ^{113}Sn decays to $^{113\text{m}}\text{In}$, which in turn decays with a half-life of 1.7 hr to the stable ground state ^{113}In , there always existed in the atomic beam a small equilibrium amount of $^{113\text{m}}\text{In}$. Furthermore, at low field the $F = I + J$, $\Delta M = 1$ flop-in transition frequency for $^{113\text{m}}\text{In}$ ($I = 1/2$, $^2\text{P}_{3/2}$ electronic state) is exactly equal to that for ^{113}Sn with $I = 1/2$ in the $^3\text{P}_1$ state. Because of this coincidence, all resonance buttons in ^{113}Sn runs were counted twice, with several 1.7-hr half-lives in between, to insure that any signal seen was not due to $^{113\text{m}}\text{In}$. In none of the runs was there any clear evidence of interference due to presence of $^{113\text{m}}\text{In}$ in the beam. It is presumed that the failure to observe $^{113\text{m}}\text{In}$ resonances was due to the poor flop-in efficiency of In ($g_J = -4/3$) compared with Sn. Since the Sn flop-in signals corresponded to transitions with $\Delta M_J = \pm 2$,

the Sn atoms were more strongly deflected by the A and B fields because of the larger change in their atomic magnetic moment. In addition, the K x-ray counting system used to detect ^{113}Sn was relatively insensitive to the 0.393-Mev γ ray emitted in the decay of $^{113\text{m}}\text{In}$.

VII. HYPERFINE-STRUCTURE MEASUREMENTS

A. Experimental Procedure

Several different types of rf transitions were observed in ^{121}Sn and ^{113}Sn at various magnetic fields in order to obtain values for the hfs interaction constants. These types are summarized in Table II.

As with all similar atomic-beam experiments, the procedure used was to proceed by extrapolation from regions of transition frequency and magnetic field where flop-in signals had been observed to new values of frequency and field where they had not. Observations of new signals then allowed further extrapolation to higher field or to another type of transition based on updated values of the interaction constants.

In accordance with the above procedure, the Type 1 transition which had been used to measure the spins was followed up in field to about 35 gauss for each of the isotopes; at this field the signal-to-background ratio had dropped considerably (from 3.5 to 0.5 for ^{121}Sn) because of the breakdown of the low-field approximation of equal Zeeman level spacing that allows observation of this transition. In order to proceed to higher values of magnetic field a two-frequency technique, involving superposition of two rf fields in the transition region, was employed. As used in the Type 2 observations, the method requires rf fields at frequencies matching the two energy intervals that make up the

Type 1 double-quantum interval. Thus one frequency corresponds to the interval $(F,M) \leftrightarrow (F,M+1)$ and the other to the interval $(F,M+1) \leftrightarrow (F,M+2)$. One then has, in effect, atoms making the Type 1 double-quantum transition $(F,M) \leftrightarrow (F,M+2)$.

The operation of the two-frequency technique can be understood qualitatively by considering a simplified three-level system as shown in Fig. 3 and the following simple argument. We wish to cause an atom in state 1 to make a transition to state 3 by superimposing two rf fields at frequencies ν_{12} and ν_{23} . The two fields are introduced into the transition region by forming their Fourier sum and applying this sum to the conductor leading to a shorted rf loop in the C magnet of the beam apparatus. Thus as an atom travels the length of the transition region it "sees" both fields simultaneously. It is possible to visualize an ideal situation with all beam atoms moving with the same velocity and the two rf field intensities so adjusted that in passing through the first half of the transition region an atom starting in state 1 has unit probability of making the transition $1 \rightarrow 2$ and in passing through the remaining half has unit probability of making the transition $2 \rightarrow 3$. Of course since the fields are superimposed, it is equally probable that in the second half of the transition region an atom would make the reverse transition $2 \rightarrow 1$; one expects half of the atoms to do this and the net result is a probability of 0.5 for the overall process $1 \rightarrow 2 \rightarrow 3$. A similar argument yields the same result for the absorption process $3 \rightarrow 2 \rightarrow 1$. Thus, to the extent that such a crude argument holds, one might expect two-frequency flop-in signals to be as large as the low-field single frequency Type 1 signal, since the argument doesn't depend

on the two frequencies being unequal. In both cases one would expect at most one half of the atoms in states 1 and 3 to contribute to the flop-in signal. This was borne out by the experimental observations; the Type 2 and 4 signals were of about the same strength as the low-field Type 1 double-quantum signals.

The implementation of the two-frequency technique required two rf generators, rf power amplifiers, a means of measuring the two frequencies, and a device for forming the Fourier sum before transmission into the transition region. Figure 4 shows a schematic diagram of the rf circuit required.

The method used, in a typical run, to locate the two peak frequencies, ν_{12} and ν_{23} , was as follows: One rf generator was set to the predicted frequency for one of the resonance peaks, say ν_{12} , and the other generator's frequency was varied until a signal corresponding to the 2 \rightarrow 3 transition was detected. This resonance line shape was then traced out so that its peak could be located to give a first measurement of ν_{23} . Once this was done the second generator was held to this peak frequency while the first was varied to improve the location of ν_{12} . This process could then be repeated until the location of the two peak frequencies no longer changed and the measurement of ν_{12} and ν_{23} at that particular magnetic field was completed. In practice it was found that one could locate ν_{12} and ν_{23} uniquely with only one or two sweeps of each resonance.

Figure 5 shows the Type 2 two-frequency resonances *b* and *c* from Run 892 in the experiments on ^{121}Sn . The levels involved in these resonances are $(F_1 = 5/2, M_1 = 5/2)$, $(F_2 = 5/2, M_2 = 3/2)$ and $(F_3 = 5/2, M_3 = 1/2)$. The peak on the right corresponds to the 1 \rightarrow 2 transition

and that on the left to the $2 \rightarrow 3$. These observations were made at a magnetic field of 24.3 gauss. This is low enough to observe a Type 1 signal with a single frequency midway between the two resonance peaks; however, as the plot shows, there is a significant difference between the peak frequencies ν_{12} and ν_{23} (about 1 MHz). This difference is a direct measurement of the effects of the hyperfine structure on the Zeeman levels.

At moderate magnetic fields, where ν_{12} and ν_{23} do not differ by more than a few line widths, it is possible for the presence of the rf field at frequency ν_{23} to shift the position of the resonance at ν_{12} from its unperturbed location by an amount $\delta\nu_{12}$ given roughly by³

$$\delta\nu_{12} = \frac{(\Gamma_{23})^2}{8(\nu_{12} - \nu_{23})}, \quad (8)$$

where Γ_{23} is the line width of the $2 \rightarrow 3$ resonance (full width at half maximum). An analogous expression holds for $\delta\nu_{23}$. The result is that the apparent separation of the $1 \rightarrow 2$ and $2 \rightarrow 3$ peaks is larger than in the unperturbed case. Calculation of the size of this effect in these measurements shows that it was small and entirely negligible, amounting to a maximum shift of 0.020 MHz for the lowest-field Type 2 observations on ^{121}Sn . This is well within the assigned error in the peak locations (0.100 and 0.075 MHz). The size of the shift for all other observations on the two isotopes was much smaller due to the increased size of $(\nu_{12} - \nu_{23})$.

For both of the isotopes studied, the Type 2 resonances were observed at various values of the C field extending up to about 200 gauss. These observations produced values for the various hfs intervals which were sufficiently precise to allow searching at near zero magnetic field for

Type 3 or Type 4 resonance signals that connect hfs levels differing in F by one. Observations of such resonances serve as direct measurements of the hfs interval except for a correction for the departure from zero field. Figures 6 and 7 show such resonances obtained for the two hfs intervals of ^{121}Sn . Figure 8 shows the $\Delta F = 1$ Type 5 resonance observed in ^{113}Sn . The measurement was made at a value of the magnetic field ($H = 115.6$ G) at which the derivative of the transition frequency with respect to magnetic field is zero. Operation at such a point minimizes C -magnet inhomogeneity as a source of line broadening.

B. Summary of Observations and Results

Figures 9 and 10 are energy-level diagrams for the 3P_1 hfs levels of ^{121}Sn and ^{113}Sn in an external magnetic field. Indicated by the vertical lines and heavy dots are the transitions observed and the states involved. The solid lines indicate single-frequency Type 1 and 3 transitions; the dashed lines indicate the two-frequency Type 2, 4, and 5 transitions.

Table III lists the quantum numbers of the observed transitions and Tables IV and V contain the experimental data. Table VI presents the final values for the hfs constants as determined by a least-squares computer fit to the data.⁴ Also included are the measured nuclear spins, the nuclear magnetic-dipole and electric-quadrupole moments deduced from the measured hfs constants, and the χ^2 of the computer fits for the two possible signs of the interaction constants. Preliminary values of these results were reported earlier.⁵

From Childs' and Goodman's measurement⁶ of a positive sign for a in the 3P_1 state of the stable isotopes $^{115}, ^{117}, ^{119}\text{Sn}$ and the known⁷

negative sign μ_I for these isotopes, it is known that a and μ_I should have opposite signs. The difference in the χ^2 values of the computer fits for the two possible sign combinations is not significant enough to establish the sign of μ_I for ^{121}Sn and ^{113}Sn from the data obtained in these experiments. However, nuclear theory strongly supports the sign choice $\mu_I(^{121}\text{Sn}) > 0$ and $\mu_I(^{113}\text{Sn}) < 0$, and accordingly Figs. 9 and 10 are drawn for negative and positive hfs constants respectively. The sign of b relative to a for ^{121}Sn was determined by these experiments to be positive.

The values for the magnetic moments were obtained from the measured spins and a constants by using the known^{6,7} values for I , μ_I , and a of ^{119}Sn and the usual Fermi-Segrè comparison relation

$$\mu_I = (I/I')(a/a')\mu_I' \quad (9)$$

The nuclear quadrupole moment q of ^{121}Sn was determined from the measured value of b and Eq. (6). For q_J the relation

$$q_J = 0.219 \langle r^{-3} \rangle \quad (10)$$

was used with $\langle r^{-3} \rangle$ given by

$$\langle r^{-3} \rangle = \xi / (2\mu_0^2 Z_{eff}^2 H) \quad (11)$$

where $\xi = 2171.5 \text{ cm}^{-1}$ is the fine-structure splitting constant determined by Childs and Goodman⁸, $Z_{eff} = 46$, and the relativistic factor $H = 1.02$.⁹ The factor 0.219 in the relation for q_J comes from a calculation of the effects of Casimir-type relativistic corrections using the effective-operator technique of Sandars and Beck;¹⁰ the nonrelativistic factor is 1/5.

The quantities in parentheses in Table VI represent the errors in the last figures quoted. For the interaction constants (a and b), this error represents one standard deviation. The errors quoted for the magnetic moments are taken as 1% to allow for a possible hfs anomaly [departure from Eq. (9)], even though such anomalies among the stable tin isotopes 115 , 117 , ^{119}Sn are known to be very small⁶ ($\leq 0.04\%$). The large error (50%) quoted for Q represents the uncertainty in the calculation of $\langle r^{-3} \rangle$ and the possibility of large configuration interaction and Sternheimer shielding effects, which have not been determined.

VIII. DISCUSSION OF SPINS AND MOMENTS

With $Z = 50$ the Sn isotopes have a closed-shell proton core and, to a large extent, the static nuclear properties should be attributable to the neutron states. ^{113}Sn and ^{121}Sn have 13 and 21 neutrons beyond the $N = 50$ closed shell, and these are distributed among the single-particle subshells $2d_{5/2}$, $1g_{7/2}$, $3s_{1/2}$, $2d_{3/2}$, and $1h_{11/2}$. The single-particle shell model then attributes the spins $I = 1/2$ for ^{113}Sn and $I = 3/2$ for ^{121}Sn to the odd neutron of the isotopes occupying the $3s_{1/2}$ and $2d_{3/2}$ subshells respectively.

These assignments yield Schmidt moments $\mu_I(s_{1/2}) = -1.913$ nm and $\mu_I(d_{3/2}) = 1.148$ nm, which are too large by factors of 2.2 and 1.6 compared with the measured values of $\mu_I(\text{corr})(^{113}\text{Sn}) = \pm 0.879(9)$ nm and $\mu_I(\text{corr})(^{121}\text{Sn}) = \pm 0.699(7)$ nm. Despite the large disparity in magnitude between the Schmidt values and the observed moments, it is improbable that the signs of the magnetic moments are other than those of the Schmidt values.

Using a δ -function perturbation on shell-model-plus-pairing-force wave functions, Freed and Kisslinger¹¹ have obtained remarkable agreement between calculated and observed magnetic moments of odd-neutron nuclei in the mass region $A = 105$ to $A = 149$. In particular, they obtain agreement to within 10% over the chain of isotopes ^{111}Cd , ^{113}Cd , ^{115}Sn , ^{117}Sn , and ^{119}Sn , all with $I = 1/2$ and magnetic moments of about -1.00 nm. Because of the smooth variation of the μ_I 's with mass over this range of $I = 1/2$ nuclei, it is expected that their treatment would have similar success with ^{113}Sn . Freed and Kisslinger did not calculate μ_I 's for $I = 3/2$ nuclei near $A = 121$, they did, however, obtain agreement to within 10% for ^{131}Xe ($I = 3/2$, $Z = 54$, $N = 77$, $\mu_I = 0.691$ nm).

Our measured value of the quadrupole moment of ^{121}Sn , $Q = \pm 0.08(4) \times 10^{-24} \text{ cm}^2$, is in fair agreement with the results of a calculation carried out by using an expression derived by Kisslinger and Sorensen,¹²

$$Q = \frac{2I-1}{2(I+1)} \langle I|r^2|I \rangle e_{eff} (U_I^2 - V_I^2) \left(1 + \frac{\chi}{C}\right), \quad (12)$$

where e_{eff} is the effective charge assigned to the odd neutrons because of their polarization of the proton core, and V_I^2 and U_I^2 give the probabilities of occupancy and nonoccupancy of the shell-model state with $j = I$ ($2d_{3/2}$ for ^{121}Sn). The quantity χ is the strength of the long-range quadrupole force between nucleons, and C is a parameter giving the strength of the coupling of the single particle to the collective motion of the odd nucleons. Schneid, Prakash, and Cohen¹³ have carried out (d,p) and (d,t) reaction studies on the even Sn isotopes, and their measurements yield

$U_{3/2}^2 = V_{3/2}^2 = 0.5$ for ^{120}Sn indicating simply two neutrons in the $2d_{3/2}$ subshell. Adding one neutron to obtain ^{121}Sn then yields the result $(U_{3/2}^2 - V_{3/2}^2) = -0.5$. For the other quantities in Eq. 12, the values¹² used were $\langle I|r^2|I\rangle = 4.0 \times 10^{-26} \text{ cm}^2$, $e_{eff} = 1$, and $\frac{\lambda}{c} = 1.5$. The calculated result is then $Q = -0.02 \times 10^{-24} \text{ cm}^2$.

ACKNOWLEDGMENTS

We acknowledge gratefully the assistance of Mr. Dana Vance and Mr. Patrick Yarnold for their help in these experiments, particularly for their patient and competent counting of the radioactive buttons. We thank also Mrs. Julia Taylor and Miss Nadine Kamada for their excellent typing of the manuscript.

FOOTNOTES AND REFERENCES

- * Research supported by the U. S. Atomic Energy Commission
- † Presently on leave at: Faculteit der Wiskunde en Natuurwetenschappen,
Katholieke Universiteit, Nijmegen, Netherlands
- ‡ Present address: Columbia Radiation Laboratory, Columbia University
New York, New York
- ¹ N. F. Ramsey, *Molecular Beams* (Oxford University Press, 1956).
- ² C. Schwartz, *Phys. Rev.* 97, 380 (1955).
- ³ N. F. Ramsey, *Phys. Rev.* 100, 1191 (1955).
- ⁴ V. J. Ehlers, et al., *Phys. Rev.*
- ⁵ M. H. Prior, H. A. Shugart, and P. A. Vanden Bout, *Bull. Am. Phys. Soc.* 12, 904 (1967); A. Dymanus, M. H. Prior, and H. A. Shugart, *Bull. Am. Phys. Soc.* 12, 1046 (1967).
- ⁶ W. J. Childs and L. S. Goodman, *Phys. Rev.* 137, A35 (1965).
- ⁷ W. G. Proctor, *Phys. Rev.* 79, 35 (1950).
- ⁸ W. J. Childs and L. S. Goodman, *Phys. Rev.* 134, A66 (1964).
- ⁹ H. Kopferman, *Nuclear Moments* (Academic Press, New York, 1958).
- ¹⁰ P. G. H. Sandars and J. Beck, *Proc. Roy. Soc. (London)* A289, 97 (1965).
- ¹¹ N. Freed and L. S. Kisslinger, *Nucl. Phys.* 25, 611 (1961).
- ¹² L. S. Kisslinger and R. A. Sorensen, *Kgl. Danske Videnskab. Selskab, Mat.-Fys. Medd.* 32, 9 (1960).
- ¹³ E. J. Schneid, A. Prakash, and B. Cohen, *Phys. Rev.* 156, 1316 (1967).

FIGURE CAPTIONS

- Fig. 1. Results of ^{121}Sn spin search; the small signal at $I = 5/2$ is actually the wing of the $I = 3/2$ resonance.
- Fig. 2. Results of ^{113}Sn spin search.
- Fig. 3. Schematic three-level diagram of energy versus magnetic field. In the A and B magnetic fields, where $\langle \mathcal{K}_Z \rangle \gg \langle \mathcal{K}_{hfs} \rangle$, the levels are characterized by the $m_J = \langle J_Z \rangle$ quantum numbers listed on the right.
- Fig. 4. Schematic diagram of rf circuit used in two-frequency runs.
- Fig. 5. Type 2 two-frequency resonances observed in ^{121}Sn at $H = 24.3$ G. The resonance labels b and c are those of Table III, where the quantum numbers associated with each are listed.
- Fig. 6. ^{121}Sn Type 4 $\Delta F = 1$ hyperfine transition resonance e at $H = 2.5$ G. The quantum numbers assigned to this resonance are listed in Table III.
- Fig. 7. ^{121}Sn Type 4 $\Delta F = 1$ hyperfine-transition resonance f at $H = 2.5$ G. The quantum numbers assigned to this resonance are listed in Table III.
- Fig. 8. ^{113}Sn Type 5 $\Delta F = 1$ resonance n at $H = 115.7$ G. The quantum numbers assigned to this resonance are listed in Table III. At this field the derivative of the frequency of this transition with respect to the magnetic field is zero.
- Fig. 9. Energy level diagram for the 3P_1 hfs levels of ^{121}Sn . The diagram is drawn for hfs constants $a, b < 0$. The value of $M = \langle F_z \rangle$ for each level is indicated along the inside border. The vertical lines and heavy dots indicate the transitions observed; solid lines are single-frequency transitions, dashed lines are two-frequency transitions.

Fig. 10. Energy-level diagram for the 3P_1 hfs levels of ^{113}Sn . The diagram is drawn with $a > 0$. The vertical lines and heavy dots indicate the transitions observed; solid lines are single-frequency transitions, dashed lines are two-frequency transitions.

Table I. Sn electronic states.

<u>State</u>	<u>Energy</u> <u>(cm⁻¹)</u>	<u>Beam Atoms</u> <u>in state</u>	<u>g_J</u> ^a
³ P ₀	0.0	52.7%	0
³ P ₁	1691.8	34.8%	-1.50110(7)
³ P ₂	3427.7	12.4%	-1.44878(9)
¹ D ₂	8613.0	0.1%	-1.05230(8)
¹ S ₀	17162.6	≈ 0	0

^a Ref. 8.

Table II. Types of transitions observed.

Type	Quantum Numbers			rf Frequencies required
	Level 1	Level 2	Level 3	
1	F, M		F, M±2	one at $\nu = (E_1 - E_3)/2h$
2	F, M	F, M±1	F, M±2	two at $\nu_{12} = (E_1 - E_2)/h$ and $\nu_{23} = (E_2 - E_3)/h$
3	F, M	F±1, M±1		one at $\nu = (E_1 - E_2)/h$
4	F, M	F±1, M±1	F±2, M	} same as Type 2
5	F, M	F±1, M	F±1, M±1	

Table III. Quantum Numbers of Observed Resonances.

Isotope	Transition Type	Resonance Label	Quantum Numbers*						
			F_1	M_1	F_2	M_2	F_3	M_3	
^{121}Sn	1	a	2.5	2.5			2.5	0.5	
	2	{ b c	2.5	2.5	2.5 2.5	1.5 1.5	2.5	0.5	
	3	d	1.5	1.5	2.5	0.5			
	4	{ e f	0.5	-0.5	1.5 1.5	0.5 0.5	2.5	-0.5	
	4	{ g h	0.5	-0.5	1.5 1.5	-1.5 -1.5	2.5	-0.5	

	^{113}Sn	1	i	1.5	0.5			1.5	-1.5
		2	{ j k	1.5	0.5	1.5 1.5	-0.5 -0.5	1.5	-1.5
3		m	1.5	0.5	0.5	-0.5			
5		{ n p	1.5	0.5	0.5 0.5	0.5 0.5	0.5	-0.5	

* Assumes $a, b < 0$ for ^{121}Sn ; $a > 0$ for ^{113}Sn .

Table IV. Experimental data ^{121}Sn .

Run No.	Calibration data		Sn Isotope data		$v_{obs} - v_{calc}$ (MHz) (g_I assumed positive)
	Isotope*	Frequency (error) (MHz)	Resonance [†] Label	Frequency (error) (MHz)	
868A	A	0.438(25)	a	1.030(25)	-0.025
871A	A	0.989(20)	a	2.352(25)	-0.039
871B	A	2.013(18)	a	4.880(25)	-0.020
871C	A	3.923(15)	a	9.618(50)	-0.050
871D	A	6.073(18)	a	15.155(15)	-0.022
872A	A	6.975(18)	a	17.515(30)	-0.017
876A	A	8.856(18)	a	22.525(30)	-0.005
891C	B	2.373(30)	a	4.350(75)	0.039
891D	B	14.289(40)	a	27.250(100)	0.127
892A	B	16.730(30)	a	32.025(67)	-0.002
892D	B	11.560(50)	c	21.350(100)	0.078
892D	B	11.560(50)	b	22.200(75)	0.010
894A	B	15.546(20)	c	28.825(80)	0.014
894A	B	15.546(20)	b	30.450(50)	-0.015
894B	B	21.747(30)	c	40.750(50)	-0.006
894B	B	21.747(30)	b	43.975(75)	0.039
894C	B	31.907(40)	c	60.975(50)	-0.021
894C	B	31.907(40)	b	67.500(50)	0.047
894D	B	45.097(25)	c	88.800(200)	0.102
894D	B	45.097(25)	b	100.200(100)	-0.038
897A	B	0.431(30)	d	362.675(30)	0.000
897B	B	0.628(30)	d	362.850(40)	-0.009
900A	B	70.128(30)	c	148.540(75)	-0.012
900A	B	70.128(30)	b	167.155(50)	0.001
900B	B	98.893(30)	c	227.075(75)	0.024
900B	B	98.893(30)	b	247.365(60)	0.028
901A	B	0.919(30)	e	121.225(40)	0.010
901A	B	0.919(30)	f	363.620(30)	0.009
901B	B	1.172(20)	e	121.515(40)	-0.015
901B	B	1.172(20)	f	363.955(30)	-0.005
901C	B	0.904(25)	g	123.325(60)	0.035
901C	B	0.904(25)	h	361.500(15)	0.003

*A = ^{133}Cs , B = ^{85}Rb [†]Resonance labels are as in Table III.

Table V. Experimental data ^{113}Sn .

Run No.	Calibration data		Sn Isotope data		$\nu_{obs} - \nu_{calc}$ (MHz) (g_I assumed negative)
	Isotope*	Frequency (error) (MHz)	Resonance [†] Label	Frequency (error) (MHz)	
931	B	1.016(90)	i	3.100(150)	0.052
950	B	2.190(70)	i	6.800(100)	0.235
952	B	3.556(140)	i	10.600(300)	-0.051
953	B	2.841(75)	i	8.600(250)	0.087
954	B	6.367(100)	i	19.000(200)	-0.039
955	B	9.463(70)	i	28.000(200)	-0.244
957	B	9.382(125)	i	28.100(200)	0.097
957A	B	9.382(125)	j	27.900(200)	0.145
957B	B	9.382(125)	k	28.500(200)	0.248
960	B	11.847(50)	i	35.350(150)	0.040
961	B	14.425(70)	i	42.900(150)	-0.030
962	B	16.783(60)	i	49.900(150)	0.021
962A	B	16.783(60)	j	49.075(75)	-0.033
962B	B	16.783(60)	k	50.525(75)	-0.094
964A	B	31.884(50)	j	91.700(75)	0.031
964B	B	31.884(50)	k	96.275(75)	0.002
965A	B	61.654(50)	j	172.600(75)	0.109
965B	B	61.654(50)	k	185.475(100)	0.145
966A	B	109.667(65)	j	297.580(75)	-0.076
966B	B	109.667(65)	k	323.150(75)	-0.107
967	B	0.466(66)	m	731.000(150)	0.035
983	A	0.515(37)	m	731.975(150)	0.014
984	A	0.595(34)	m	732.425(100)	-0.018
1003B	C	83.835(85)	n	687.188(50)	0.006
1004	C	83.921(85)	n	687.175(50)	-0.007

*A = ^{133}Cs , B = ^{85}Rb , C = ^{87}Rb .

†Resonance labels are as in Table III.

Table VI. Results

Isotope	Nuclear spin	hfs Constants*	Nuclear moments [†] (uncorr)	χ^2	Number of Observations
^{121}Sn	3/2	a = $\pm 128.726(8)$ MHz b = $\pm 32.374(12)$ MHz b/a > 0	$\mu_I = \mp 0.695(7)$ nm Q = $\pm 0.08(4)$ barn	$\left\{ \begin{array}{l} (+a) \ 5.21 \\ (-a) \ 4.48 \end{array} \right\}$	32
^{113}Sn	1/2	a = $\pm 485.911(25)$	$\mu_I = \mp 0.875(9)$	$\left\{ \begin{array}{l} (+a) \ 4.51 \\ (-a) \ 6.32 \end{array} \right\}$	25

*Errors represent one standard deviation.

[†] μ_I errors are 1% to allow for hfs anomaly. Error in Q is 50% to include inaccuracies in calculation of $\langle 1/r^3 \rangle$ and effects of Sternheimer shielding.

Table VII. Constants Used in Computations

Isotope	Electronic State	Spin	g_J	h.f.s a (MHz)	μ_I (uncorr) (n.m.)
^{119}Sn	$3P_1$	1/2	-1.50110(7) ^a	578.296 ^b	-1.0409 ^{c d}
^{85}Rb	$2S_{1/2}$	5/2	-2.002332(2) ^e	1011.910813(2) ^f	1.3479 ^{g h}
^{87}Rb	$2S_{1/2}$	3/2	-2.002332(2) ^e	3417.341307(2) ^f	2.7408 ^h
^{133}Cs	$2S_{1/2}$	7/2	-2.002542(2) ^e	2298.1579425 ⁱ	2.5641 ^d

$\mu_o/h = 1.399613 \text{ MHz/Gauss}$
 $M_p/M_e = 1836.12$

^aReference 8.

^bReference 6.

^cReference 7.

^dI. Lindgren, Arkiv Fysik 29, 553 (1965).

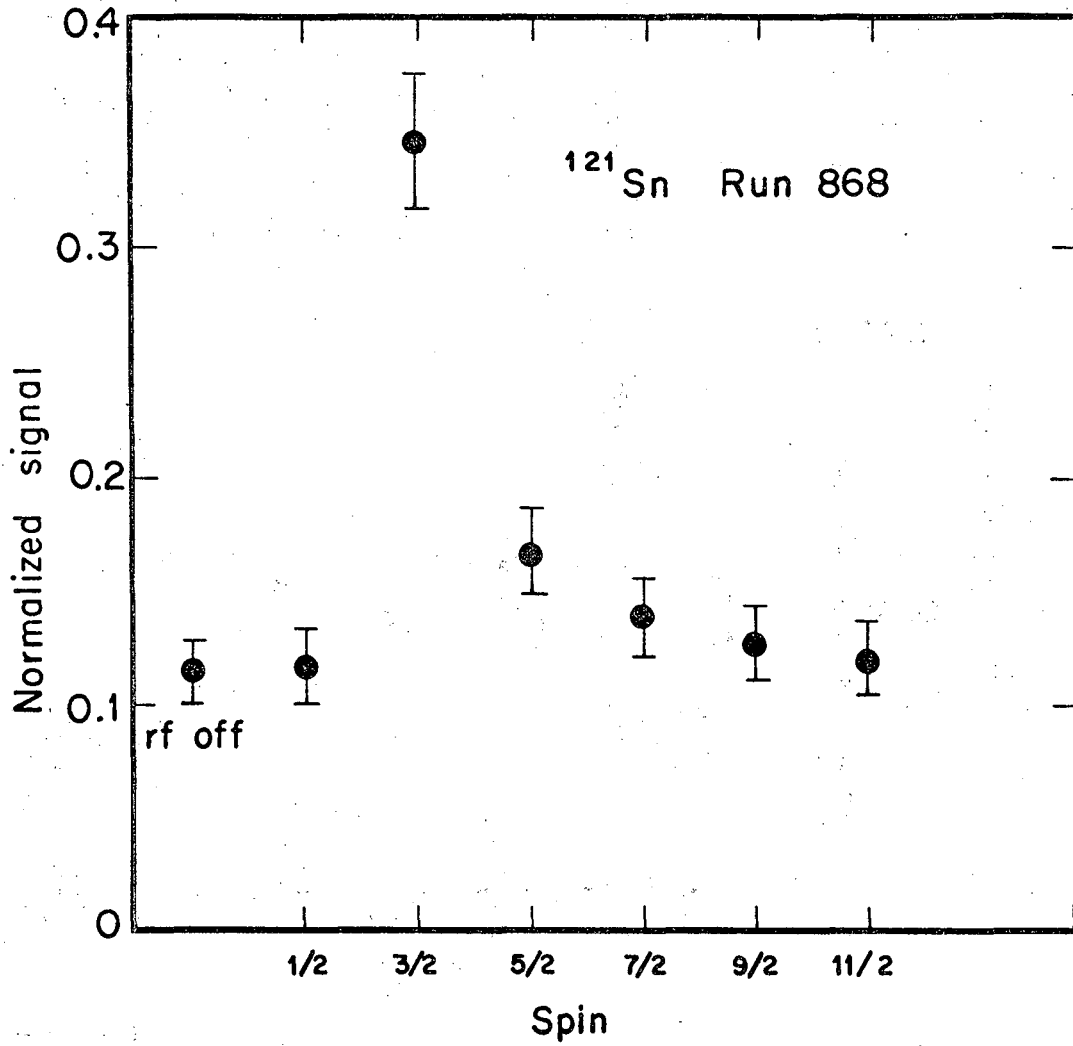
^eP. A. Vanden Bout, et al., Phys. Rev. 165, 88 (1968).

^fS. Penselin, T. Moran and V. W. Cohen, Phys. Rev. 127, 524 (1962).

^gV. J. Ehlers, T. R. Fowler, and H. A. Shugart, Phys. Rev. 167, 1062 (1968).

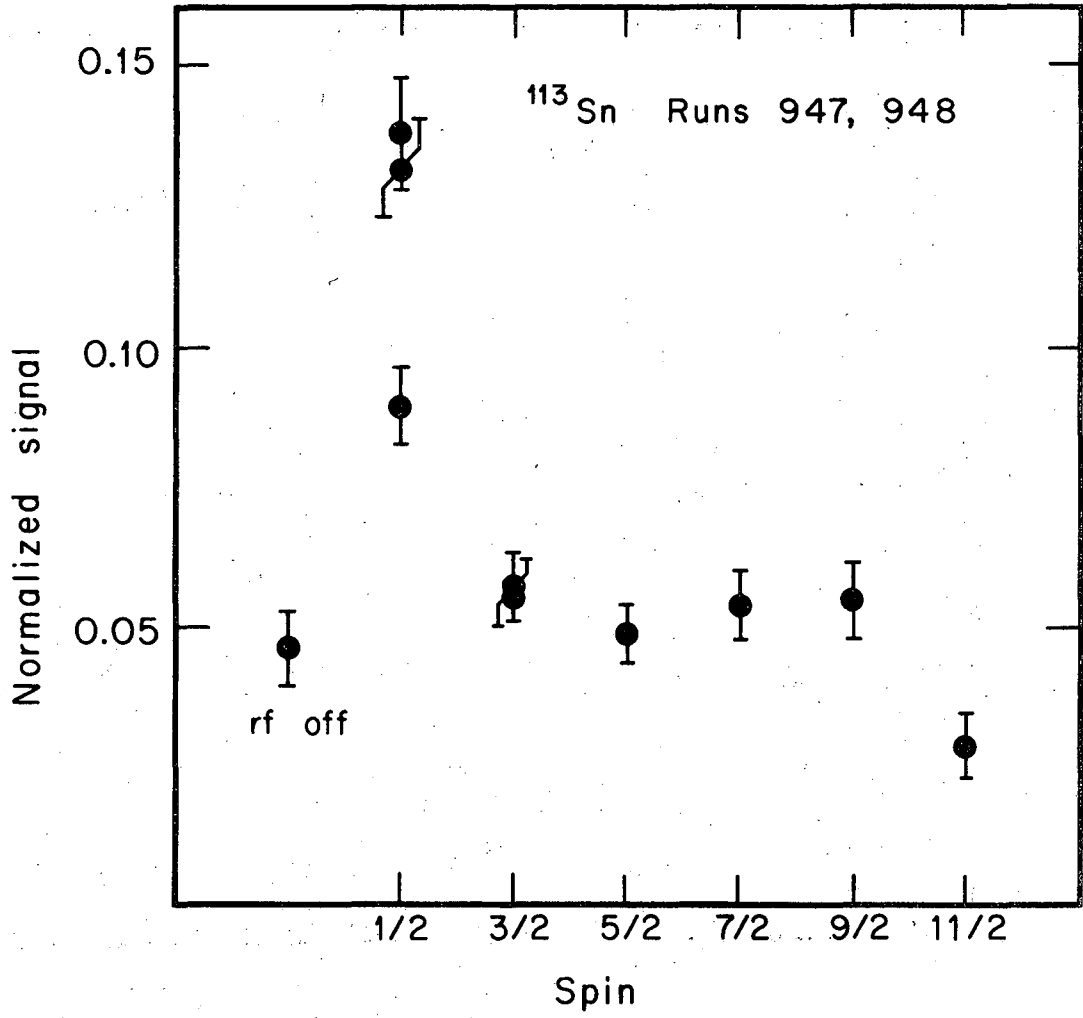
^hC. W. White, W. M. Hughes, G. S. Hayne, and H. G. Robinson, Phys. Rev. 174, 23 (1968).

ⁱThis value defines the atomic time scale.



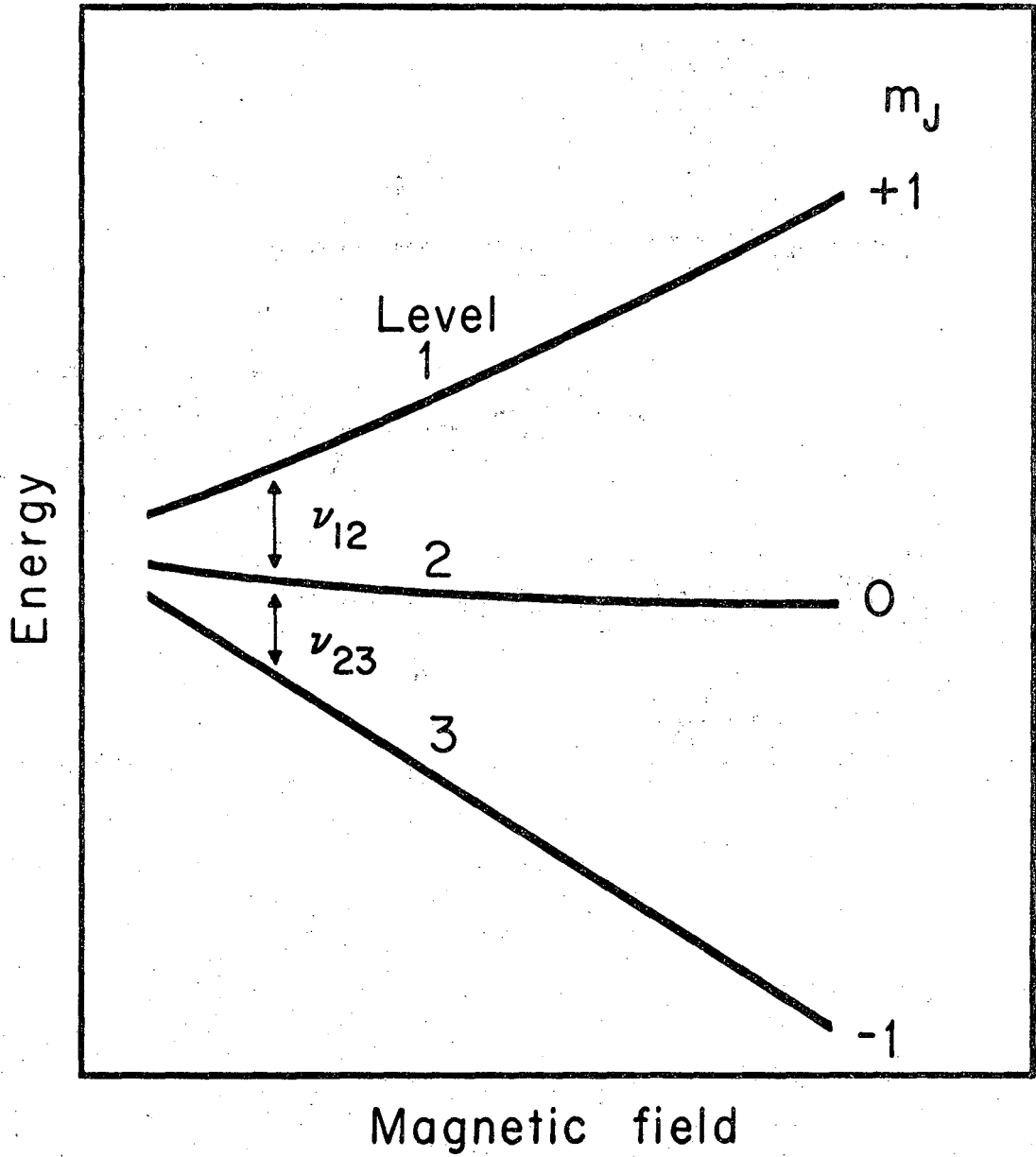
XBL674-2753A

Fig. 1



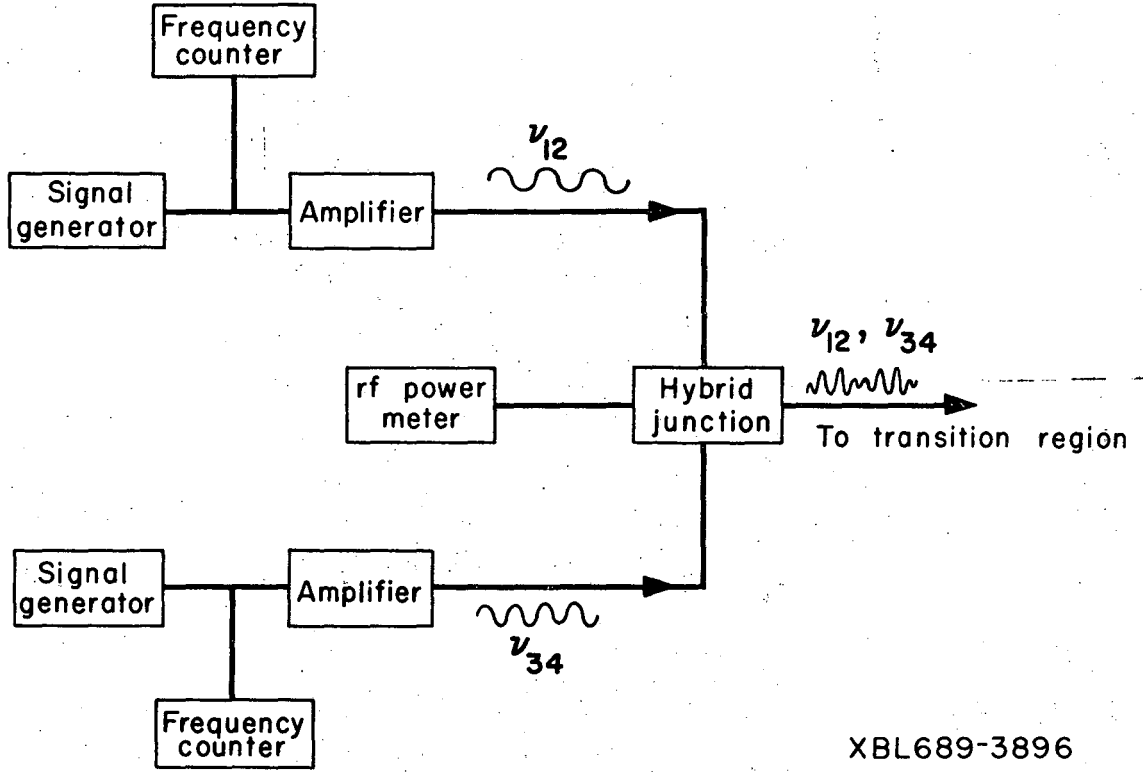
XBL689-3894

Fig. 2



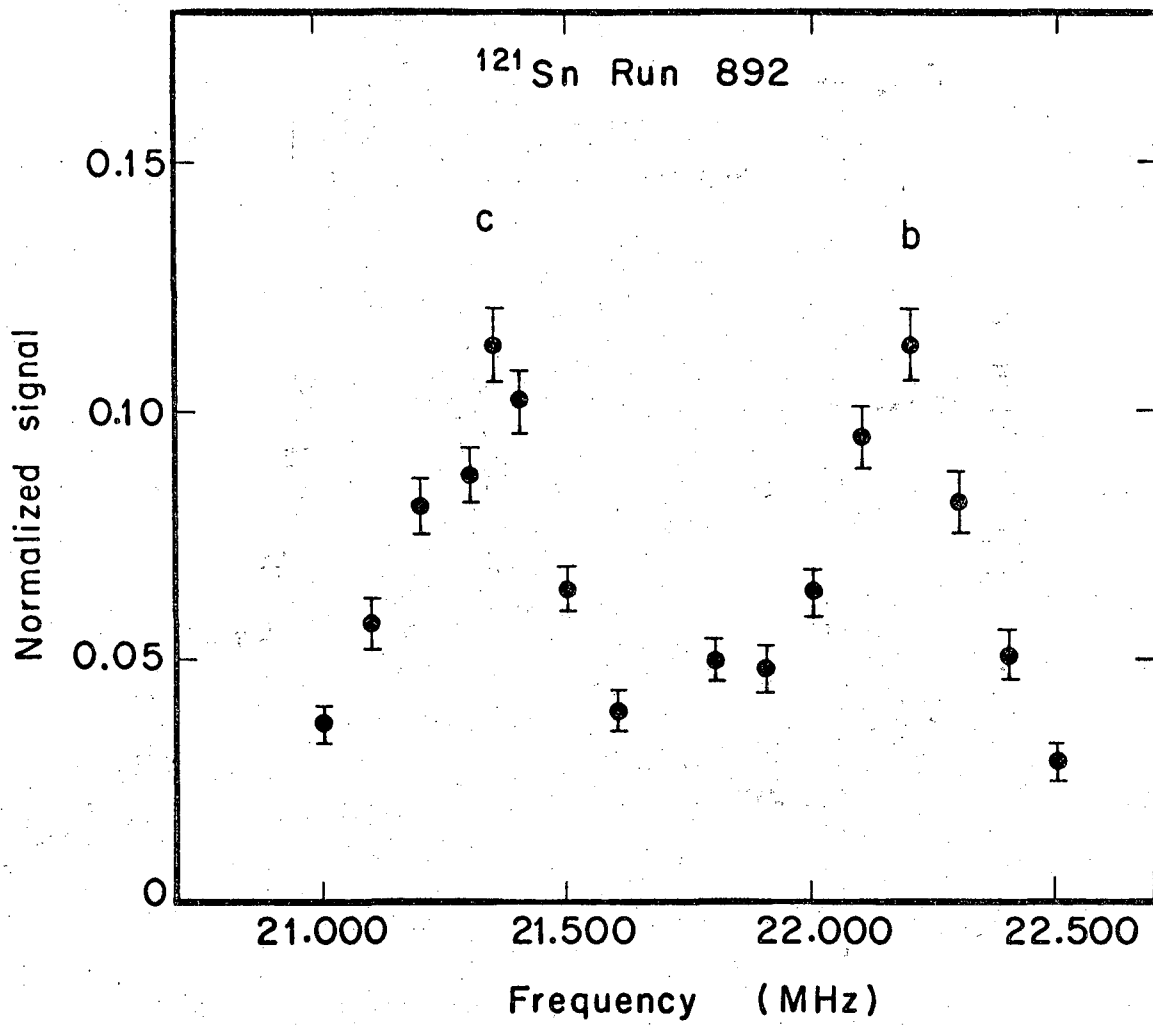
XBL689-3895

Fig. 3



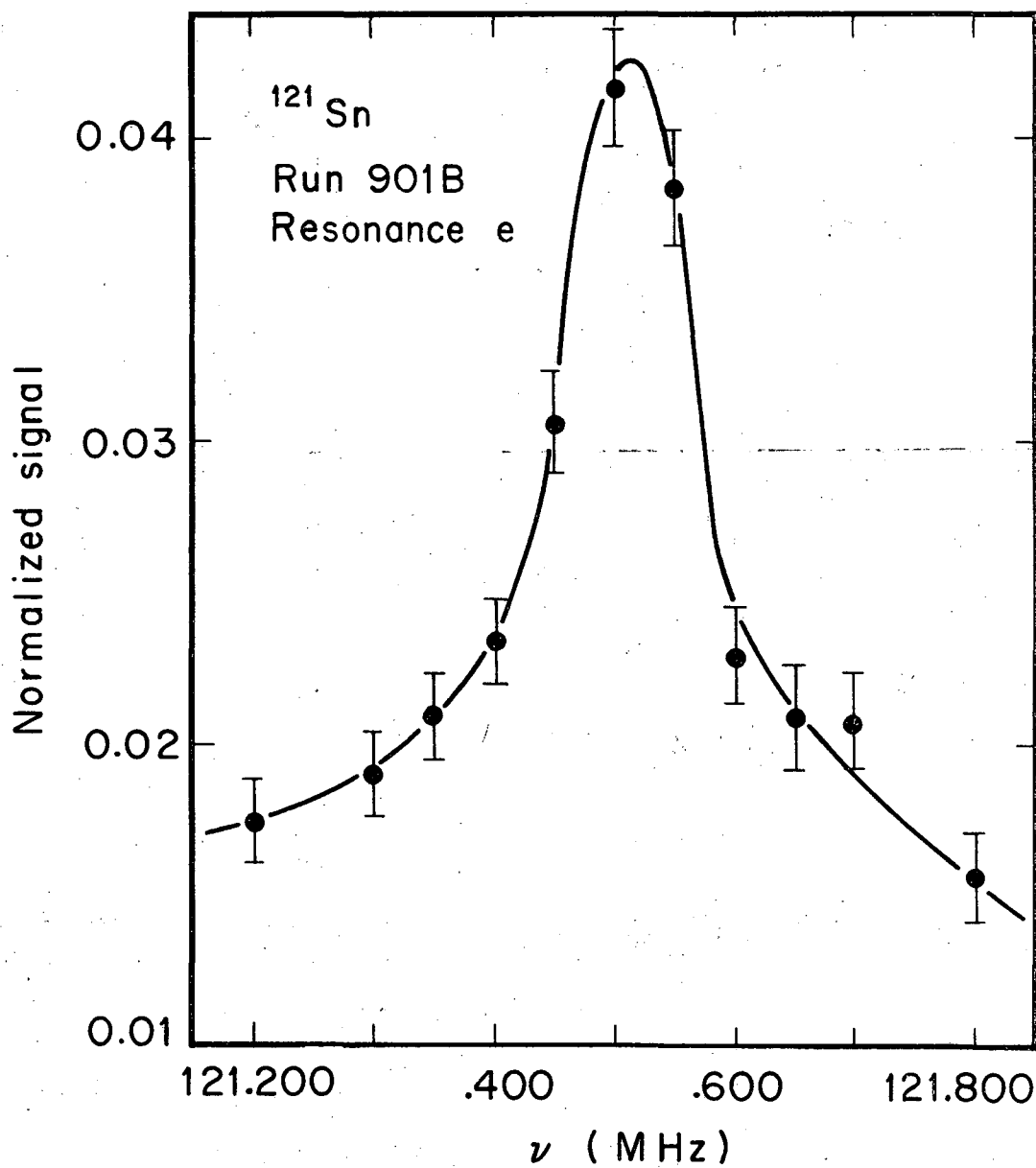
XBL689-3896

Fig. 4



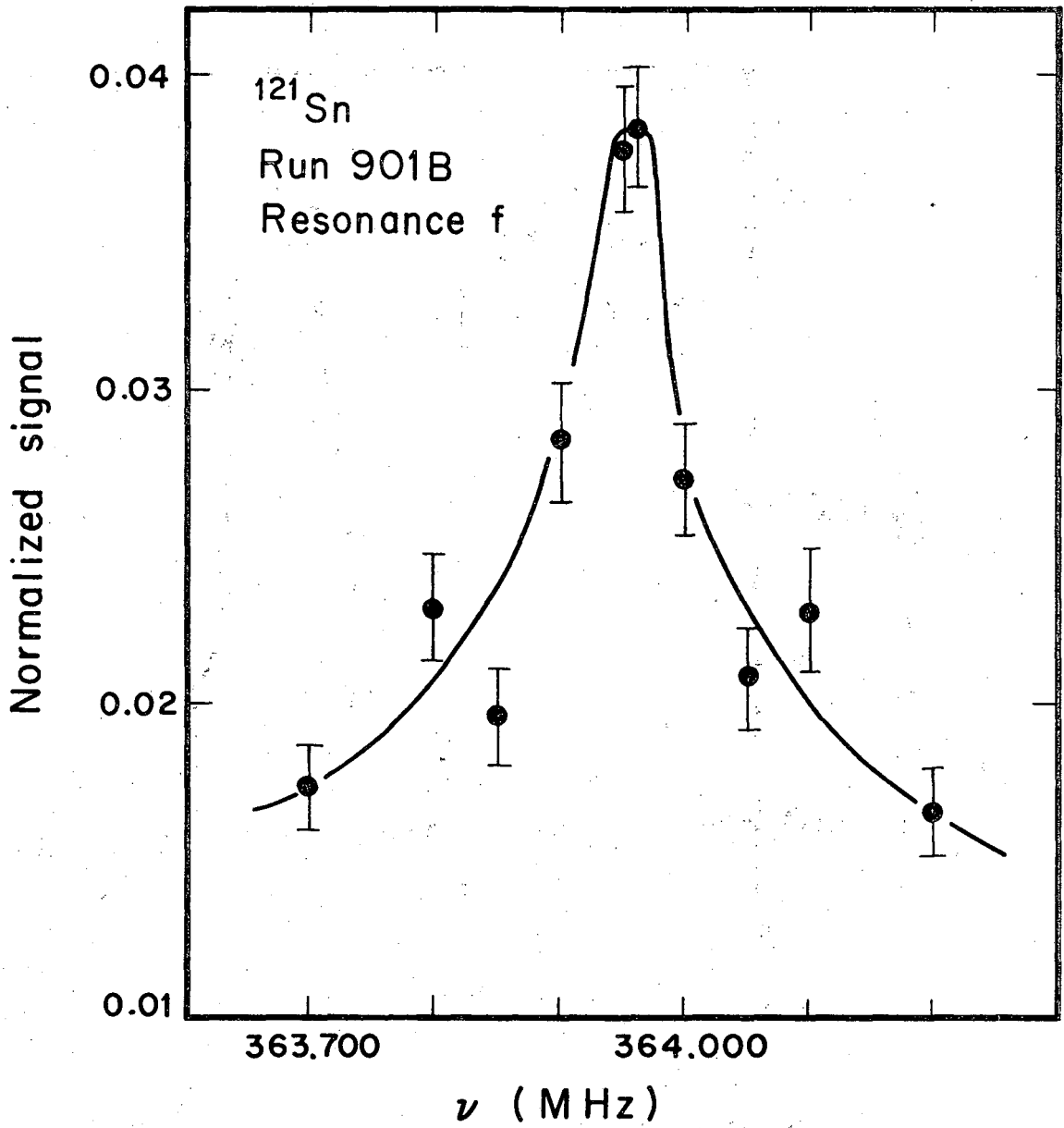
XBL674-2758A

Fig. 5



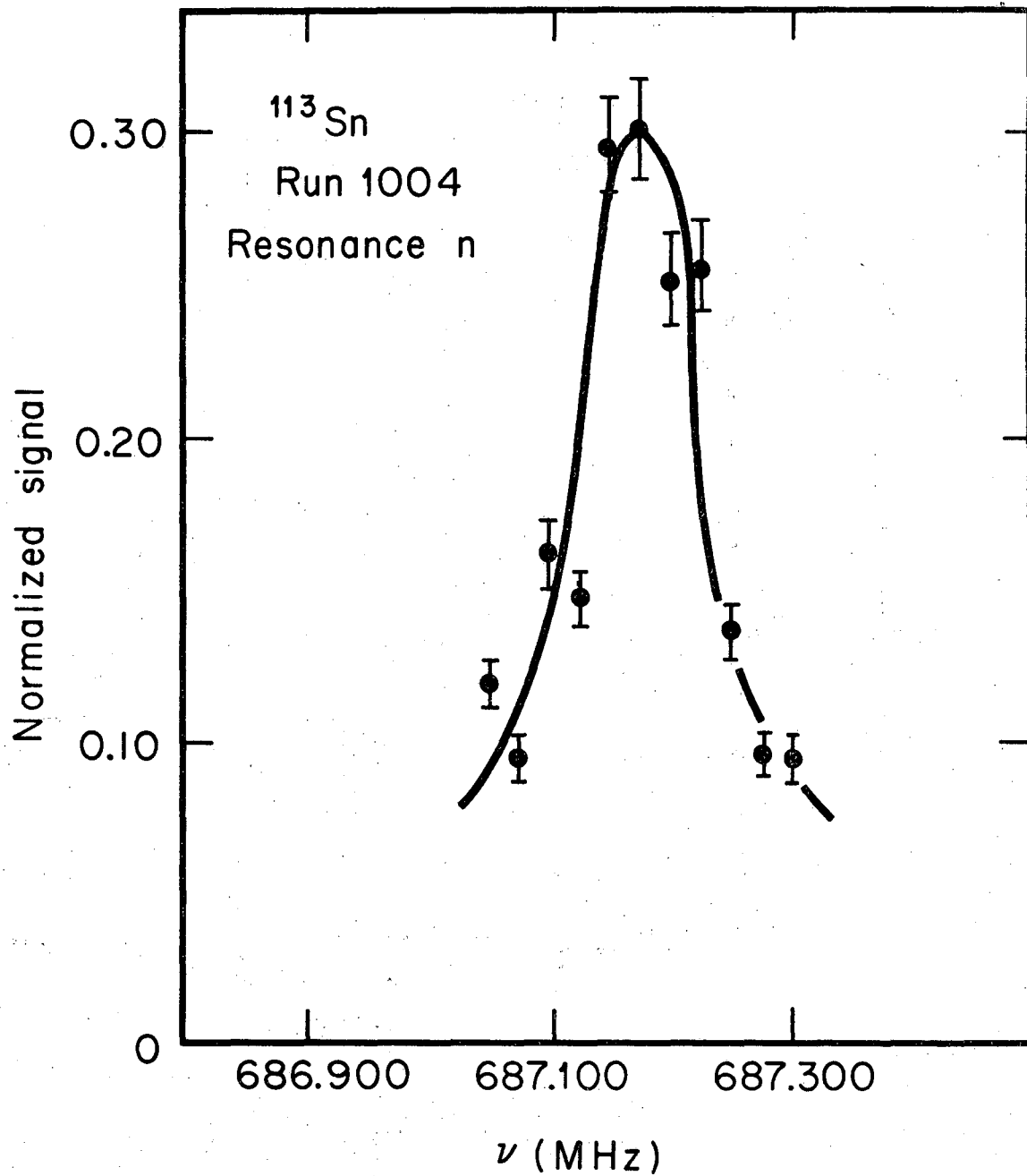
XBL674-2763A

Fig. 6



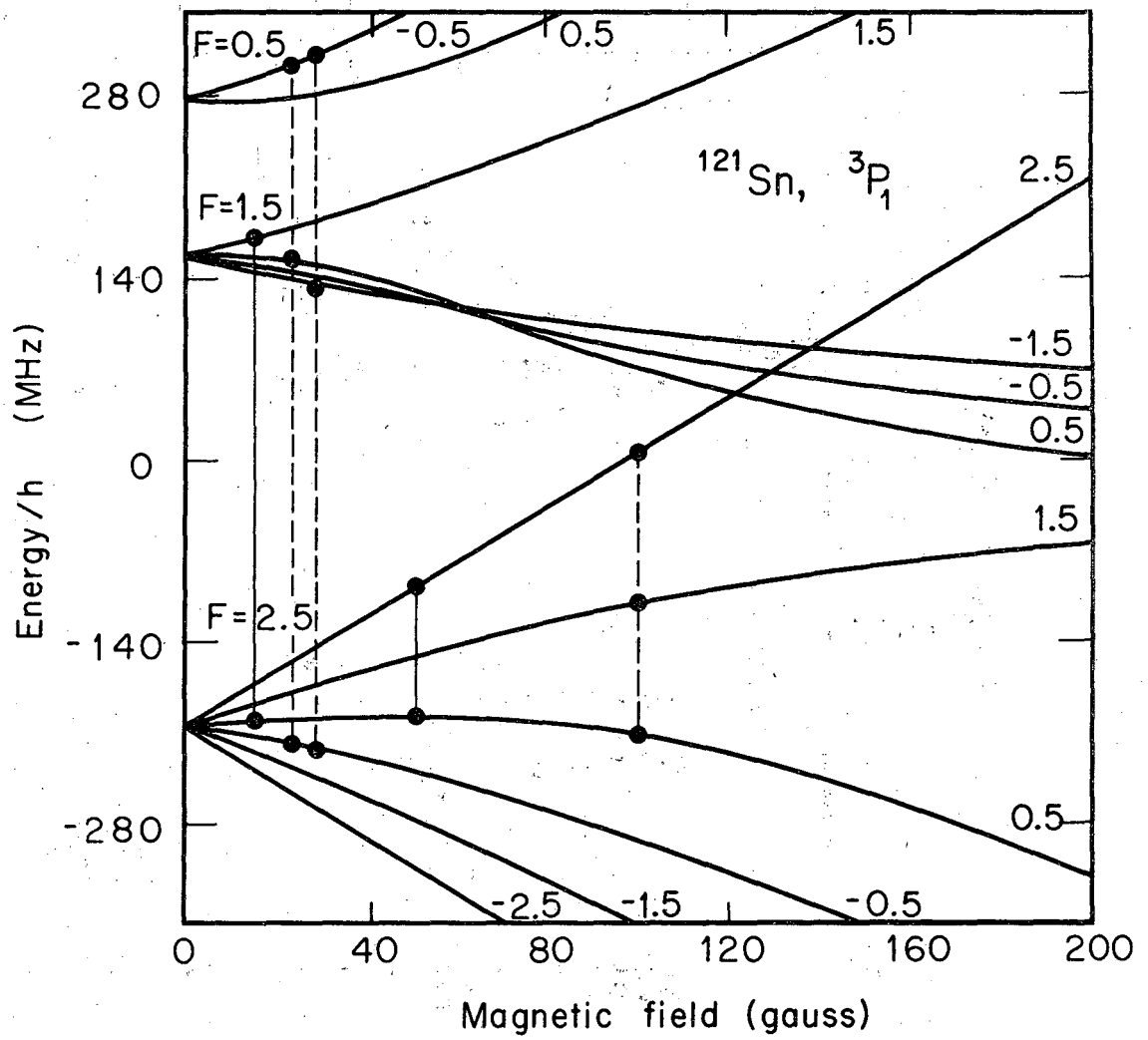
XBL674-2764A

Fig. 7



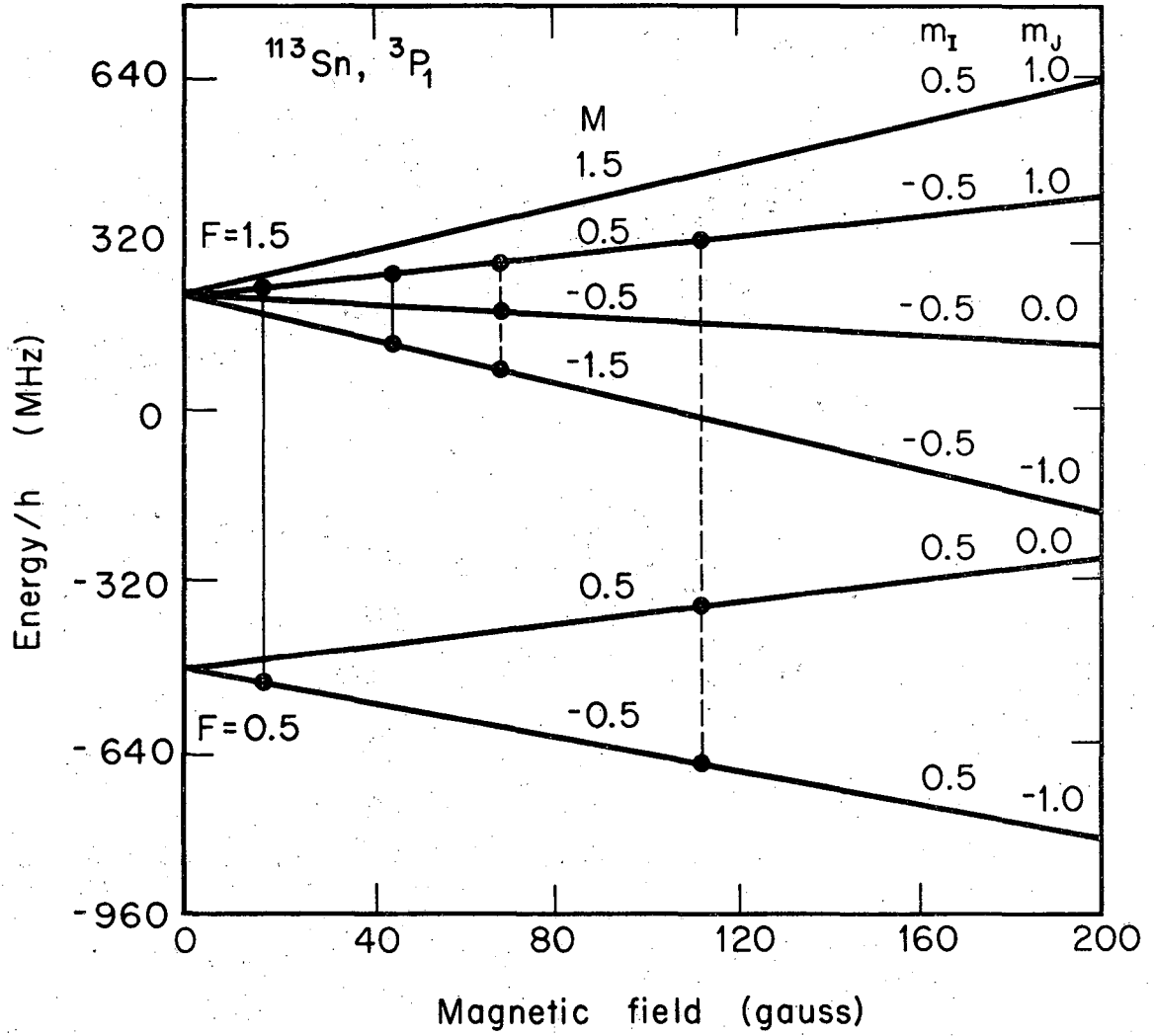
XBL 6711-6010-A

Fig. 8



XBL 689-3897

Fig. 9



XBL689-3898


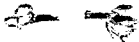
Fig. 10

LEGAL NOTICE

This report was prepared as an account of Government sponsored work. Neither the United States, nor the Commission, nor any person acting on behalf of the Commission:

- A. Makes any warranty or representation, expressed or implied, with respect to the accuracy, completeness, or usefulness of the information contained in this report, or that the use of any information, apparatus, method, or process disclosed in this report may not infringe privately owned rights; or*
- B. Assumes any liabilities with respect to the use of, or for damages resulting from the use of any information, apparatus, method, or process disclosed in this report.*

As used in the above, "person acting on behalf of the Commission" includes any employee or contractor of the Commission, or employee of such contractor, to the extent that such employee or contractor of the Commission, or employee of such contractor prepares, disseminates, or provides access to, any information pursuant to his employment or contract with the Commission, or his employment with such contractor.



TECHNICAL INFORMATION DIVISION
LAWRENCE RADIATION LABORATORY
UNIVERSITY OF CALIFORNIA
BERKELEY, CALIFORNIA 94720